Physica D 238 (2009) 1241–1255

Contents lists available at ScienceDirect

Physica D

journal homepage: www.elsevier.com/locate/physd

Coarsening and self-organization in dilute diblock copolymer melts and mixtures

Karl Glasner [a,*], Rustum Choksi [b]

[a] Department of Mathematics, University of Arizona, United States
[b] Department of Mathematics, Simon Fraser University, Canada

ARTICLE INFO

Article history:
Received 18 August 2008
Received in revised form
2 March 2009
Accepted 9 April 2009
Available online 22 April 2009
Communicated by Y. Nishiura

Keywords:
Diblock copolymers
Ostwald ripening
Coarsening
Self-organization

ABSTRACT

This paper explores the evolution of a sharp interface model for phase separation of copolymers in the limit of low volume fraction. Particles both exchange material as in usual Ostwald ripening, and migrate because of an effectively repulsive nonlocal energetic term. Coarsening via mass diffusion only occurs while particle radii are small, and they eventually approach a finite equilibrium size. Migration, on the other hand, is responsible for producing self-organized patterns.

We construct approximations based upon an ansatz of spherical particles similar to the classical LSW theory to derive finite dimensional dynamics for particle positions and radii. For large systems, kinetic-type equations which describe the evolution of a probability density are constructed. For systems larger than the screening length, we obtain an analog of the homogenization result of Niethammer & Otto [B. Niethammer, F. Otto, Ostwald ripening: The screening length revisited, Calc. Var. Partial Differential Equations 13-1 (2001) 33–68]. A separation of timescales between particle growth and migration allows for a variational characterization of spatially inhomogeneous quasi-equilibrium states.

Ostwald ripening, a coarsening process described by the exchange of material between particles of the minority phase in binary mixtures (cf. [1,2]), has been the topic of extensive study over the last 20 years. Much of the analytical work is based upon the Cahn–Hilliard equation which was conceived to model phase separation in binary alloys (cf [3]). This equation describes spinodal decomposition of a fine grained mixture and nucleation of phases rich in each component of the mixture. This is followed by interface coarsening via the Mullins–Sekerka law, which produces coarsening behavior with a well-established rate of $t^{1/3}$, i.e. the length scale of increases as a power law with exponent 1/3.

In the dilute regime, the minority phase forms particles which interact through mass diffusion, and the resulting process is termed Ostwald ripening. One can derive both finite-dimensional dynamics of individual particles, and in the limit of large particle number kinetic-type statistical descriptions ([4,5,1,2,6] and references therein). These descriptions provide a counterpart to rigorous upper bounds (e.g. [7,8]) which predict and confirm temporal scaling laws.

The Cahn–Hilliard approach applies equally well to phase separation of mixtures or melts of *homogeneous* polymers which are thermodynamically incompatible [9]. Block copolymers, on the other hand, are inhomogeneous chain molecules composed of two or more monomer types (see Fig. 1 top). Below a critical temperature, weak local repulsion of different species induces phase separation. Complete separation does not occur, however, because of molecular attachment of distinct monomer chains. Instead, a remarkable array of locally periodic "metastable" states appear: lamellar, cylindrical, spherical, gyroid structures have all been observed [10,11]. Because of their variable architecture, these materials are extremely versatile, having applications in nanotechnology, lithography, photonics and controlled drug delivery [10]. The regime of interest here is the spherical phase that is encountered for highly asymmetric mixtures. Recent experiments [12] and computational studies [13] have illuminated the dynamic processes of this phase, including defect motion and coarsening of ordered domains through grain boundary motion.

This paper studies the modification to the usual coarsening process that results from long range interactions in systems of block copolymers. Our approach is via a *modified* Cahn–Hilliard equation which arises as a gradient flow (with respect to the H^{-1} metric) of a nonlocal Cahn–Hilliard-type functional first introduced by Ohta and Kawasaki in [14]. We are interested in the strong segregation regime wherein A/B interfaces are rather sharp in comparison to domain size, and hence focus on the sharp interface limit of this equation (cf. [15])in the case of low volume fraction. That is, we consider diblock copolymers of very small molecular weight (ratio of B monomers to A) and envisage either a melt of such diblock copolymers (cf. Fig. 1, bottom left) or a mixture/blend of such diblocks with homopolymers of either type

* Corresponding address: Department of Mathematics, University of Arizona, 617 N Santa Rita, Tucson, AZ 85721, United States. Tel.: +1 520 621 4764.
E-mail addresses: kglasner@math.arizona.edu (K. Glasner), choksi@math.sfu.ca (R. Choksi).

0167-2789/$ – see front matter © 2009 Elsevier B.V. All rights reserved.
doi:10.1016/j.physd.2009.04.006

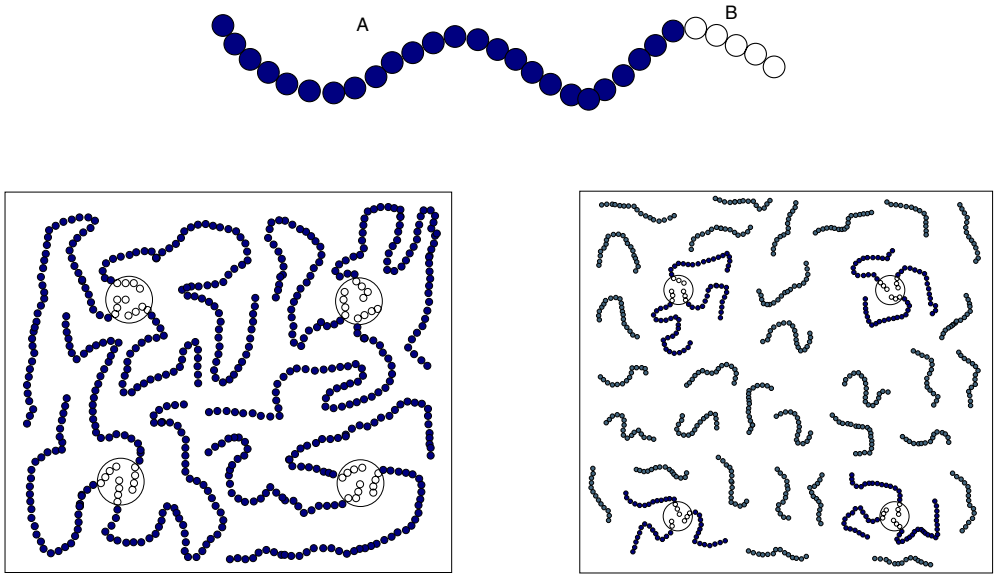

Fig. 1. Top: an AB diblock copolymer macromolecule of small molecular weight. Bottom left: microphase separation of these diblock copolymers. Bottom right: phase separation in a mixture/blend of diblock copolymers and homopolymers of another monomer species having relatively weak interactions with the A and B monomers.

A or of type *C* but for which the *CA* and *CB* interactions are relatively weak (cf. Fig. 1, bottom right).

This paper uses a plan of attack tangential to that for mixtures described by the ordinary Cahn–Hilliard equation. Sagui & Desai [16] considered an abstract prototypical model for these systems in two dimensions and studied the reduced dynamics numerically. We follow a similar reduction scheme specialized to the copolymer case in three dimensions, and go ever further to characterize the evolution statistically. In particular, we base our analysis upon an ansatz of small spherical regions (inclusions) for the minority monomer phase and utilize the following program:

(i) We identify two spatial scales, the *screening length* and the *structure length*, and the temporal regimes relevant for the evolution process of small spherical domains. The *screening length* is, roughly speaking, the distance over which particles interact and hence its relation to the sample size is important. The *structure length* is the intrinsic scale set by the competition of short and long range interactions which comprise the free energy. The temporal scales correspond respectively to traditional Ostwald ripening (coarsening), structure formation when the size of the inclusions stabilizes, and particle migration or pattern formation. Based upon the size of screening length relative to the sample size, we focus on two separate scenarios: unscreened and screened systems.

(ii) For the unscreened case, we modify the classical LSW (for Lifshitz & Slyozov [4] and Wagner [5]) theory to derive systems of effective ordinary differential equations for both the radii and the centers of the small spheres. These ODEs capture both the separation of time scales as well as the length scale corresponding to the structured regime. We characterize these equations variationally by connecting them to a reduced free energy.

(iii) For screened systems, we again apply the LSW arguments to derive ODEs for the particle radii and a kinetic equation for the particle radii distribution. We also perform a homogenization of the Poisson equation relating the potential to the spatial distribution on particles. This allows for an effective homogenized system which couples the kinetic equation with the homogenized Poisson equation, and extends a homogenization result of Niethammer & Otto [6]. One can then study stability of steady states of this system under certain constraints via a *homogenized energy*.

(iv) To address the last stage of particle migration, we develop the basic approximations one step further, which allows for additional approximation of the free energy to include a particle interaction term. We explore the consequence of this subdominant term on particle migration and pattern formation.

Our results are consistent with a recent Gamma-convergence study [17] of free energy in the small volume fraction limit, and a recent study [18] of stable local minimizers for small volume fraction limit. The Gamma-convergence study is based on the small volume fraction asymptotics of the (suitably rescaled) free energy, and reveals at leading order, a local energy responsible for the first stages of particle evolution, i.e., the coarsening process. At the next order, one finds an interaction energy responsible for the last stage of particle migration, i.e., self-organization. We discuss the connections in Sections 3.4 and 5.2.

1. The Modified Cahn–Hilliard model and its sharp interface limit

A density function theory [14,19] for the relative monomer fraction $u : \Omega \to [0, 1]$ yields a free energy of the form

$$F(u) = \int_\Omega \frac{\epsilon^2}{2}|\nabla u|^2 + W(u) + \frac{\sigma}{2}|\nabla v|^2 \mathrm{d}x \tag{1}$$

$$\Delta v = u - \rho, \qquad \rho = \frac{1}{|\Omega|}\int_\Omega u \mathrm{d}x$$

where the second term is a double-well local energy preferring $u = 0$ and $u = 1$, and the last term describes nonlocal interactions while conserving volume fraction ρ. Dynamical models can be built using a mass-conserved gradient descent method. The most natural of which is gradient flow within the Hilbert space H^{-1}, and leads to the following modification of the well-known Cahn–Hilliard equation

$$u_t = \Delta(-\epsilon^2 \Delta u + W'(u)) - \sigma(u - \rho). \tag{2}$$

The singular limit $\epsilon \to 0$, $\sigma \sim \epsilon$ is of particular interest [15,20,21], and as first noted by Nishiura and Ohnishi, it leads to a free boundary evolution which we will use as a point of departure.

Let the physical domain Ω be divided into two non-overlapping phase domains Ω^+, Ω^- where Ω^+ will denote the minority phase. The free boundary, denoted $\partial\Omega^+$, evolves according to

$$\Delta v = \gamma \begin{cases} 1-\rho & \text{in } \Omega^+ \\ -\rho & \text{in } \Omega^- \end{cases} \tag{3}$$

$$v = \kappa \quad \text{on } \partial\Omega^+ \tag{4}$$

$$V_n = [\partial v/\partial n]_+^- \tag{5}$$

where the convention is used that the normal velocity V_n and mean curvature κ are outward with respect to Ω^+. For simplicity, we take $\Omega = [0,1]^3$ and assume periodic boundary conditions throughout. The volume fraction of the dilute phase is $|\Omega^+| = \rho$; we will be concerned about the case $\rho \ll 1$.

The free energy corresponding to (3)–(5)[1] is

$$F = \int_{\partial\Omega^+} \mathrm{d}A + \frac{\gamma}{2}\int_\Omega |\nabla w|^2 \mathrm{d}x, \tag{6}$$

where w is a continuously differentiable solution (unique up to a constant) of

$$\Delta w = \begin{cases} 1-\rho & \text{in } \Omega^+ \\ -\rho & \text{in } \Omega^-. \end{cases} \tag{7}$$

The free boundary problem has a gradient flow structure; in particular

$$\frac{\mathrm{d}F}{\mathrm{d}t} = -\int_\Omega |\nabla\mu|^2 \mathrm{d}x \tag{8}$$

where $\mu = v - \gamma w$; physically μ is the chemical potential that gives rise to the material flux $-\nabla\mu$.

2. Scaling regimes of the low-volume fraction limit

We suppose that the minority phase is described to a good approximation by a collection of non-overlapping spheres (hereafter "particles")

$$\Omega^+ = \cup_{i=1}^N B_{R_i}(x_i).$$

The validity of this starting point hinges on two conditions: (1) spherical particles are, in some sense, stable equilibria, and (2) relaxation to these equilibria is faster than the dynamics of particle–particle interaction. Since the energy is nonlocal, it is impossible to regard an isolated particle as an equilibrium of the complete free boundary problem. However, in the low volume fraction limit, the energy of interaction between particles is subdominant to the particles "self-energy", and a simplified variational problem for equilibrium and stability can be considered (see Appendix A).

Let R be the typical sphere radius and d the minimum pairwise distance (see Fig. 2). We assume throughout that $R \ll d$ which implies that we are in the small volume fraction regime:

$$\rho \sim (R/d)^3 \ll 1.$$

There are two other derived length scales which distinguish the regimes to be investigated.

2.1. Spatial scales

One important scale is the screening length ξ, which roughly sets the distance over which particles interact. From a mathematical point of view, screening arises in solving elliptic Dirichlet problems in domains which are highly "perforated". It is understood that Green's functions on these domains have an exponentially decreasing character [22], with ξ setting the length scale of exponential decrease. Niethammer & Otto [6] show that the screening length for the dilute particle scenario scales as

$$\xi \sim \frac{\mathrm{d}^{3/2}}{R^{1/2}} \sim (NR)^{-1/2}$$

where N is the number of particles per unit volume. In our problem, interactions are screened when the screening length is similar or less than the system size. We later show how this length scale arises naturally in our formal approximations.

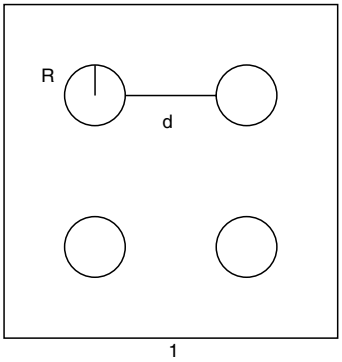

Fig. 2. Collection of particles with fixed small volume fraction ($\sim R/d$) where R denotes the radius of the spheres and d, the separation distance, and sample size is set to unity.

A second scale is set by the competition between local and nonlocal effects encoded in the parameter γ. The (non-dimensional) length $\gamma^{-1/3}$ sets the scale for the radii of near-equilibrium particles. In particular, we show that particle sizes typically approach a radius $R_* = (3/\gamma)^{1/3}$, which is smaller than the threshold R_s for stability. The relative size of R and $\gamma^{-1/3}$ therefore delineates two regimes that are characterized by the dominant balance of terms in (3).

Outside of the particle regions Ω_+, the solution v to (3) varies over scales comparable to ξ. This implies the scaling

$$\Delta v \sim \frac{R^{-1}}{\xi^2} \sim d^{-3}.$$

If

$$R \ll \gamma^{-1/3} \quad \text{(Coarsening regime)}$$

dominant balance in Ω_- gives $\Delta v = 0$, and the situation is similar to the usual description of Ostwald ripening. The other case to consider is

$$R \sim \gamma^{-1/3} \quad \text{(Structured regime)}$$

where dominant balance in Ω_- gives $\Delta v = -\gamma\rho$. This situation is predominantly characterized by equilibration of particle radii to a range of stable values, rather than coarsening.

2.2. Scaling in time

There are several temporal regimes, each characterized by a certain scaling:

- **Coarsening:** when $R \ll \gamma^{-1/3}$, the dynamics coincide with traditional Ostwald ripening, where the relevant timescale is $\tau \sim R^3$.
- **Structure formation:** when $R \sim \gamma^{-1/3}$, particle sizes equilibrate (at least locally). This equilibration also occurs on the timescale $\tau \sim R^3$. We will derive approximations on this timescale which describe relaxation of particle radii to locally

[1] Alternatively, the free energy is, modulo a constant, the Γ-limit of (1) as ϵ tends to 0 where $\sigma = \epsilon\gamma$.

constant values. Steady states of this evolution do not correspond to minimizers of the exact energy (6), but rather to low energy states which are energy minimizers of a restricted problem that ignores particle migration. In the case of small screening length, there can be a spatially inhomogeneous ("polydisperse") distribution of particle sizes. A similar interplay between spatial distribution and size was described in numerical experiments of Sagui & Desai [16].

- **Pattern formation:** This stage of evolution is described by particle migration and organization of roughly periodic patterned states, principally resulting from repulsive nonlocal energy terms. The relevant timescale is $\tau \sim Rd^3$.

3. Unscreened systems

We first describe the approximate dynamics in the simplest case when the screening length is large compared with the system size. The particle number and inter-particle distance therefore have the scales

$$N \sim d^{-3} \sim \xi^{-2}R^{-1} \ll R^{-1}. \tag{9}$$

The intermediate coarsening behavior can be captured by modifying the classical LSW theory (developed independently by Lifshitz & Slyozov [4] and Wagner [5]).

3.1. The LSW argument and its modification

Provided the radii satisfy $R \ll \gamma^{-1/3}$, dominant balance in Eq. (3) means that in Ω^-, v satisfies the Laplace equation $\Delta v = 0$ to leading order. The traditional LSW approximation assumes a spatially infinite domain; here we adjust the argument using the modified Green's function G_p that formally satisfies

$$-\Delta G_p(x) = \delta(x) - 1/|\Omega| \tag{10}$$

subject to periodic boundary conditions (Appendix B provides a review of the Ewald method for practical computation of this Green's function). Note that G_p behaves like the free space Green's function in the near field:

$$G_p(x - x_i) = \frac{1}{4\pi|x - x_i|} + O(1), \quad |x - x_i| \to 0. \tag{11}$$

The fundamental approximation takes the form

$$v(x) = A_0 + \sum_{i=1}^{N} A_i G_p(x - x_i) + O(1), \quad R \to 0. \tag{12}$$

where the coefficients A_0, A_i are assumed to be $O(R^{-1})$, $O(1)$ respectively for small R. In light of (10), there is a solvability constraint on the coefficients

$$\sum_{i=1}^{N} A_i = 0, \tag{13}$$

which guarantees $\Delta v = 0$. The validity of the ansatz (12) in the context of Ostwald ripening has been the subject of recent work (cf. [2,6]). In general, one should regard this as an "outer" or mean-field solution valid away from the free boundaries. At leading order, however, (12) also satisfactorily describes the boundary layer near each particle. The case of particle migration (Section 5), on the other hand, requires a correction term to the boundary layer.

Applying the boundary condition on v and using (11) gives asymptotically for small R

$$\frac{2}{R_i} = A_0 + \frac{A_i}{4\pi R_i} + \sum_{j\neq i}^{N} A_j G_p(x_i - x_j) + O(1). \tag{14}$$

We can estimate the size of the summation by observing that for roughly homogeneous distributions of particles, it behaves like an integral

$$\sum_{i\neq j}^{N} A_j G_p(x_i - x_j) \approx \frac{1}{d^3}\int_{\Omega} A(x)G_p(x_i - x)\mathrm{d}x = O(d^{-3}) = O(R^{-1}) \tag{15}$$

where $A(x_i) \approx A_i$. By virtue of (9), the dominant part of (14) is

$$\frac{2}{R_i} = A_0 + \frac{A_i}{4\pi R_i}. \tag{16}$$

For each particle in the minority phase Ω^+, $\Delta v \approx \gamma$, and the solution has the form

$$v(x) = C_0 + \gamma|x - x_i|^2/6, \quad x \in B_{R_i}(x_i). \tag{17}$$

In the context of the approximation, the free boundary velocity given by (5) is radially symmetric at leading order, and gives the dynamics of the particle radii as

$$\frac{\mathrm{d}R_i}{\mathrm{d}t} = [\partial v/\partial n]^-_+ \approx -\frac{A_i}{4\pi R_i^2} - \frac{\gamma R_j}{3} \tag{18}$$

For $R \ll \gamma^{-3}$, the second term in (18) is also small, leading to

$$\frac{\mathrm{d}R_i}{\mathrm{d}t} = \frac{R_i A_0 - 2}{R_i^2}. \tag{19}$$

Using (13) and (16) and summing over i leads to

$$A_0 = \frac{2N}{\sum_{i=1}^{N} R_i}. \tag{20}$$

Eqs. (19) and (20) are the traditional LSW approximation, which only holds in our system for large screening lengths and radii much smaller less than the structure length scale.

When $R \sim \gamma^{-1/3}$, dominant balance yields the Poisson equation $\Delta v = -\gamma\rho$ in the exterior region Ω^-. The monopole ansatz (12) can still be used, but the solvability condition on the coefficients changes:

$$v(x) \approx A_0 + \sum_{i=1}^{N} A_i G_p(x - x_i), \qquad \sum_{i=1}^{N} A_i = -\gamma\rho. \tag{21}$$

Using (16) and the fact that $\gamma \sim R^{-3}$, it follows that to leading order

$$\frac{\mathrm{d}R_j}{\mathrm{d}t} = \frac{R_j A_0 - 2 - \gamma R_j^3/3}{R_j^2} \tag{22}$$

Summing over all i in (16) and using the solvability constraint in (21) leads to

$$A_0 = \frac{2N}{\sum_{i=1}^{N} R_i} + \frac{\gamma}{3}\frac{\sum_{i=1}^{N} R_i^3}{\sum_{i=1}^{N} R_i}. \tag{23}$$

Eqs. (22) and (23) are a modification of the traditional LSW approximation in the structured regime. The remainder of this section will discuss their behavior.

3.2. Behavior of the modified LSW evolution

The system (22) and (23) reduces to the classical LSW approximation for $\gamma = 0$. In that case, $A_0/2$ is the reciprocal of the average particle radius, and the interpretation of (22) is simple:

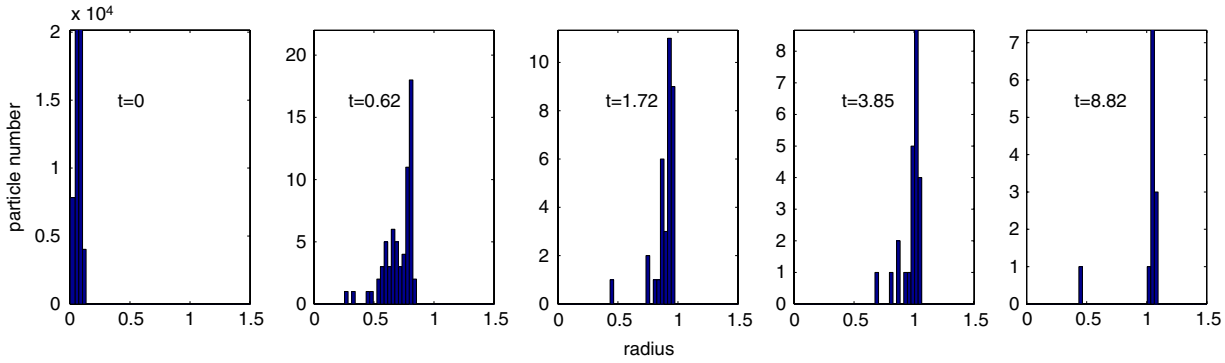

Fig. 3. Evolution of the reduced dynamics of Eqs. (22) and (23). There were initially 10^6 particles with radii chosen from a uniform random distribution of $R \in [0, R_*/10]$. The critical radius was chosen to be $R_* = 1$. Toward the end of the simulation (rightmost frame) most particles have radii near R_*. Eventually all radii converge to the same value (not shown).

particles larger than the average will grow, while the smaller ones will shrink.

The situation for $\gamma > 0$ is more involved. From the form of (22) it is clear that particles which are very small or large relative to the average will shrink, whereas particles with radii in the "growth" interval

$$I_g(A_0) = [R_-(A_0), R_+(A_0)],$$
$$R_\pm \text{ are positive roots of } R_j A_0 - 2 - \gamma R_j^3/3$$

have $\mathrm{d}R/\mathrm{d}t \geq 0$. Note that this interval cannot be empty, otherwise all radii would shrink and volume would not be conserved.

3.2.1. Small particle initial conditions

Suppose that initially all particle radii are very small, so that the first term in the expression for A_0 dominates. As coarsening proceeds, A_0 will diminish along with the size of the interval I_g. Ultimately, most particles will have either vanished or have radii close to this shrinking interval, which is itself vanishing as a critical value A_0^* of A_0 is approached. Near this point, most particles must have similar radii which will converge to a common value R_* when the interval I_g just vanishes. This happens when the growth rate $R_* A_0 - 2 - \gamma R_*^3/3$ undergoes a saddle-node bifurcation (relative to the parameter A_0), given by

$$R_* A_0^* - 2 - \gamma R_*^3/3 = 0, \qquad \frac{\mathrm{d}(R_* A_0^* - 2 - \gamma R_*^3/3)}{\mathrm{d}R_*} = 0, \tag{24}$$

which has the solution $A_0^* = \gamma R_*^2$ where the critical radius is

$$R_* = \left(\frac{3}{\gamma}\right)^{1/3}.$$

Of course, a small fraction of particles may have radii larger than the growth interval. These particles will lose mass as particles in I_g grow. If these two sets of particles reach equilibrium before I_g vanishes, then the equilibrium radius may be somewhat larger than R_*. This possibility is investigated more deeply by considering energetic stability (Section 3.3).

To illustrate the behavior for small particle initial conditions, we have simulated (22) and (23) with particles sizes chosen from a uniform random distribution in the interval $R \in [0, R_*/10]$. The reported behavior is more or less the same for any randomization. After a transient period, the particle radii distribution is peaked, and the average particle radius increases until it is just slightly larger that R_* (Fig. 3). We also compute the average radius (Fig. 4). Initially, the coarsening process follows the expected LSW scaling, but saturates when particle sizes are on the same order as the structural length.

Fig. 4. Average radius for the evolution (22) and (23) with small particle initial conditions. The dashed line with slope 1/3 is provided for comparison. Initially, the usual coarsening scaling $R \sim t^{1/3}$ is observed, but slows when radii are comparable to R_*.

3.2.2. Arbitrary initial conditions

If radii are not all small initially, there may be a substantial fraction above the growth interval I_g. Ultimately most radii should converge to a common value $\bar{R} \approx R_+(A_0)$ since particles just bigger than $R_+(A_0)$ will shrink, while those just smaller will grow. This is possible for any value of $\bar{R}$ which is the larger of the two roots of $f(R) = RA_0 - 2 - \gamma R^3/3$, which can be shown to satisfy

$$\bar{R} \geq \left(\frac{3}{\gamma}\right)^{1/3} = R_*. \tag{25}$$

There is therefore a range of stable long term behavior depending on initial conditions, characterized by convergence of particle radii to a common radius $\bar{R} \geq R_*$.

Simulations of (22) and (23) for arbitrary initial conditions show similar coarsening of small particles (Fig. 5), but the average radius converges to a value somewhat larger than R_* (Fig. 6).

3.3. Energetic reasoning

The behavior described above can also be explained in terms of an approximation of the system energy. In particular, we can show that within the context of the LSW approximation, an assembly of particles of common radius R is energetically stable if and only if $R \geq R_*$.

The self-energy of an isolated, spherical particle of radius R can be regarded as the sum of the surface energy $4\pi R^2$ and the nonlocal contribution in (6). The solution to (7) for $\rho \approx 0$ is approximated in a way similar to v. The difference is that instead of a Dirichlet